ELSEVIER

Journal of Alloys and Compounds 328 (2001) 84–89

Journal of ALLOYS AND COMPOUNDS

www.elsevier.com/locate/jallcom

Invited original talk

On the band structure of HgTe and HgSe — view from photoemission

C. Janowitz[a,*], N. Orlowski[a], R. Manzke[a], Z. Golacki[b]

[a]*Humboldt-Universität zu Berlin, Institut für Physik, Invalidenstr. 110, 10115 Berlin, Germany*
[b]*Institute of Physics, Polish Academy of Sciences, Al. Lotnikow 32/46, 02-668 Warsaw, Poland*

Received 17 September 2000; received in revised form 20 December 2000; accepted 22 December 2000

Abstract

The electronic structure of the Hg-chalcogenides HgTe and HgSe was studied by means of high resolved photoemission along the $\Gamma\Sigma K$-direction with the aim of investigating prototype materials for the inverted band structure model in detail. The samples were prepared by cleavage of the non polar (110)-surface plane to minimize the effects of surface charges. Assuming free electron parabola for the final states and considering reciprocal umklapp vectors the bulk band structure of the complete valence band was determined. This enabled a comparison to a state of the art–theoretical band structure calculation and to older experimental results obtained with different methods. In the case of HgTe with large spin–orbit splitting also the individual Γ_7, Γ_6, and Γ_8-bands could be resolved at the valence band maximum, confirming the model of the inverted band structure directly. An attempt was made to apply this direct method also to HgSe.

Keywords: Highly resolved photoemission: Zero bandgap semiconductors; Bandstructure

PACS: 79.60.BM; 73.61.Ga; 71.20.Nr; 79.60.i

1. Introduction

The electronic structure of zero gap semiconductors has become a matter of discussion recently since by a combination of photoemission and inverse photoemission a positive fundamental gap for HgSe(100) has been found by Gawlik et al. [1]. This has raised the general question on the validity of the inverted band structure model, initially discovered by Piotrzkowski [2] for mercury based II–VI semiconductor compounds, an important issue, for this model has so far been underlying the physics of this semiconductor family. In the following, these findings have stimulated intensive discussions [3] and new experimental and theoretical work [4,5].

In this contribution beneath, the study of HgTe, which can be viewed as the prototype of the mercury based semiconductors, also comparisons to reference compounds like CdTe and to the non-polar (110) cleavage face of HgSe will be made to arrive at a comprehensive picture by an enlarged set of experimental photoemission data. An investigation of nonpolar faces is advantageous because no surface charge exists for defect free cleaves and therefore no band bending, i.e. flat band conditions can be expected. Due to the fact that the uppermost valence band region is made up of chalcogene atoms, the larger spin–orbit splitting of Te as compared to Se (0.9 and 0.3 eV, respectively) makes an identification of individual bands much easier for the former material. While the spin–orbit split bands were used for HgTe(110) for a proof of the inverted band structure [6], this direct method is not appropriate for HgSe(110). Instead the dispersion of the bands over an enlarged portion of the Brillouin zone will be used for discussion.

2. Experimental

Photoemission measurements were performed at room temperature and partially at cryogenic temperature (40 K) with synchrotron radiation in the range $h\nu = 10 \ldots 30$ eV from the DORIS III storage ring at the HONORMI beamline of Hamburg Synchrotron Radiation Laboratory (HASYLAB) in Hamburg and at the 3mNIM1 beamline of the BESSY I storage ring in Berlin, both equipped with a 3 m normal incidence monochromator and electron spectrometers with high energy and angular resolution consist-

*Corresponding author. Tel.: +49-30-2093-7739; fax: +49-30-2093-7729.

E-mail address: christoph.janowitz@physik.hu-berlin.de (C. Janowitz).

0925-8388/01/$ – see front matter
PII: S0925-8388(01)01350-0

ing of a hemispherical electron energy analyzer mounted on a two-axes goniometer. The overall energy resolution was below 100 meV, the angular resolution depending on the spectrometer used was better than 1°. The Fermi energy was determined by photoemission from a polycrystalline gold film evaporated onto a plate of copper attached to the sample holder.

HgTe crystals were grown by a modified Bridgman technique at the Polish Academy of Sciences in Warsaw. Quality and orientation were checked by X-ray diffraction. The crystals were cut into pieces of $3\times3\times2$ mm^3 size and were cleaved in ultrahigh vacuum by the anvil and wedge technique along the (110) surface, at liquid nitrogen temperature, resulting in flat surfaces. As was pointed out by Yu et al. [7], extrinsic surface core level shifts at the spin–orbit split Hg5d bands can be observed in photoemission spectra in the case of poor cleavage. We never observed this effect in our spectra, so it is concluded that we always had good surface quality which was occasionally also confirmed by the observation of sharp LEED patterns (Fig. 1). The concentration of dopants as determined by SIMS remained below 2.2 and 1.7×10^{18}/cm^3 for Cu and Ni respectively.

In the case of HgSe the same preparation and characterization methods were used. Since Fe is known to function as a resonant donor with its energy level below the conduction band minimum [8,9], an influence on the spectra could not be excluded. A maximum concentration of 5.7×10^{19} of Fe was detected by SIMS, being just 0.3 atomic percent of the Hg-atom concentration and by a factor of 43 less than in the crystals used by Orlowski et al. [9]. Accordingly the effects on the photoemission spectra are expected to be less important. Overall the HgTe(110)-cleaves were of better quality than the (110)-cleaves of HgSe. In the latter case both, reasonable LEED pictures but also pictures with additional spots pointing to a disturbed surface were observed. Under the microscope a group of parallel planes with their long side parallel to the (100) direction was found. One possible reason are crystalline inhomogenities.

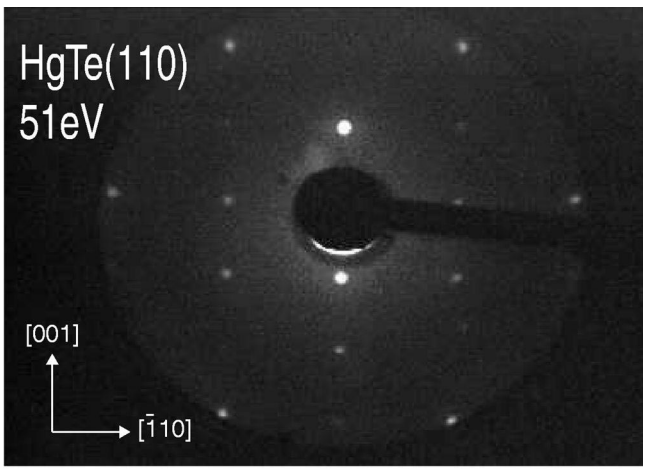

Fig. 1. LEED pattern at 51 eV of HgTe(110) prepared by cleavage.

3. Band structure determination

In order to determine the experimental band structure within the model of nearly free-electron like final states the spectra are fitted by a sum of Gaussian lineshapes and a Shirley type background while taking the spectrometer function and the Fermi–Dirac-distribution into account. In this way for each peak the kinetic energy is determined and by use of the wave vector formula $k_\perp = \sqrt{2m/\hbar^2(E_{kin}+|V_0|) - G_\parallel^2} - G_\perp$ the experimental band structure $E_b(k_\perp)$ between Γ and K is obtained, by choosing appropriate reciprocal lattice vectors $\vec{G}$ that may be composed of reciprocal bulk and surface lattice vectors.

4. Photoemission on HgTe(110)

Fig. 2 shows a selection of energy distribution curves taken at room temperature in normal emission in the photon energy range $h\nu = 8.3 \ldots 24$ eV, i.e. along the Σ line of the bulk Brillouin zone. The binding energy is refered to the valence band maximum that is found for $h\nu = 23$ eV in agreement with Ref. [10].

At the utilized photon energies strong emission structures from the Γ point can normally be described by $G = 2\pi(220)/a$ where $a = 6.462$ Å is the lattice constant of HgTe at room temperature. In this way the inner potential is determined to $V_0 = -10.3$ eV. Using this value together with the reciprocal lattice vectors $2\pi/a(220)$, $2\pi/a(111)$, $2\pi/a(200)$, $2\pi/a(020)$, $2\pi/a((220)+(001))$ and $2\pi/a((200)+(001))$ the experimental band structure between Γ and K is obtained which is shown in Fig. 3.

For comparison a theoretical ab initio band structure [11] (solid lines) is also given in Fig. 3. In general there is very good agreement for all bands. Also the band width of the theoretical band structure is close to what is found experimentally. The most obvious deviation between experiment and theory is found for the light hole band near the Γ-point. The energetic position of this band determines the negative fundamental band gap E_g. Of course, the theoretical band structure is calculated for $T = 0$ K while the measurements were performed at room temperature. As result $E_g(300\ \text{K}) = -0.32\pm0.03$ eV is obtained experimentally. Compared to $E_g = -0.14$ eV as derived by a compilation of magnetooptical results [13] this value is much larger. Additionally we performed photoemission for the upper valence band regime at room temperature and at $T = 40$ K, the latter is depicted in Fig. 4. Only for very accurately oriented samples and at very good vacuum conditions the splitting of the topmost peak and its dispersion to the Fermi level at 23 eV photon energy could

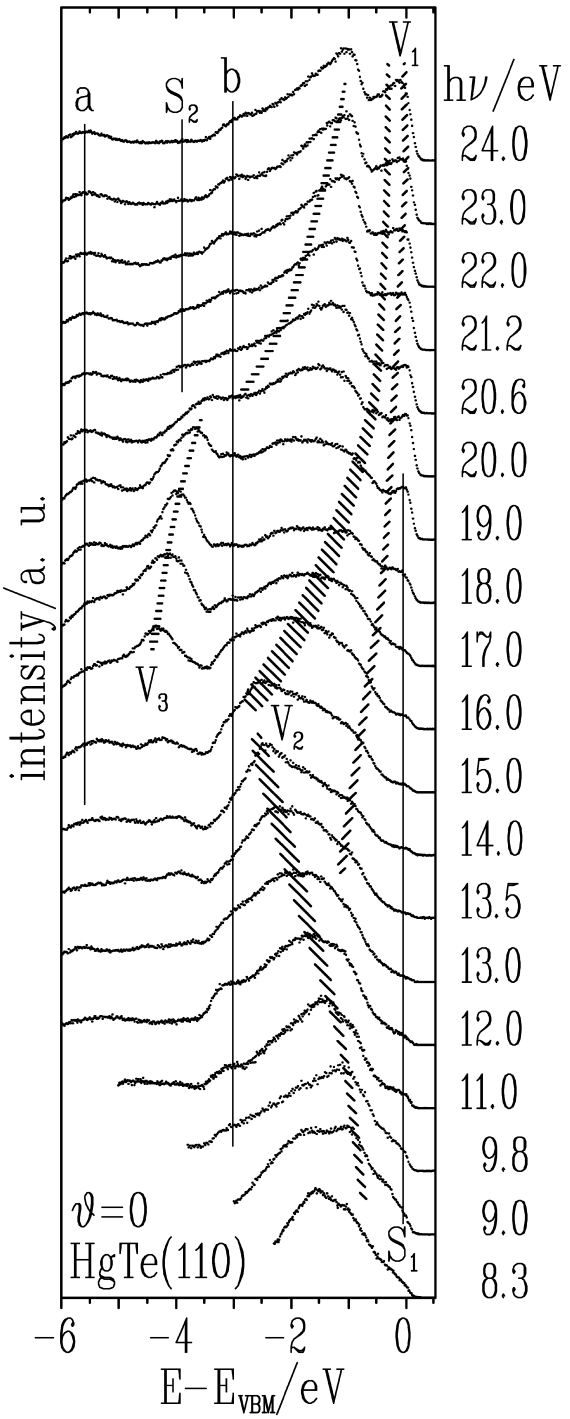

Fig. 2. Energy distribution curves in normal emission of HgTe(110). The shaded structures show dispersion and are related to bulk state emissions, straight lines denote surface state derived features.

be observed. A detailed study on this was given by Orlowski et al. [6]. Furthermore all three bulk bands Γ_7, Γ_6 and Γ_8 were detected giving additional evidence of the inverted band structure.

The obtained spin–orbit splitting Δ of 910 meV co-

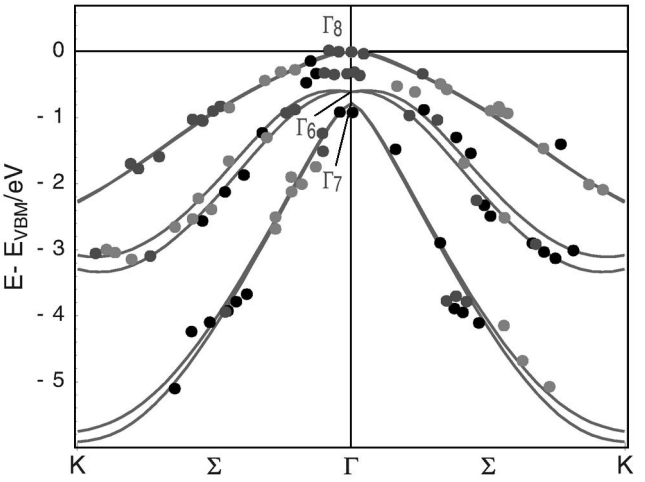

Fig. 3. Experimental band structure (points, the grey scale represents the validity of the obtained peak positions) compared with an ab initio calculation.

incides well with the corresponding value on CdTe(110) [12], also obtained by photoemission. The photoemission value $E_g(40\ \mathrm{K}) = -0.29 \pm 0.02$ eV for the negative gap compares well with the result of magnetooptical measurements [13]. From photoemission therefore a negative temperature coefficient $\mathrm{d}(E(\Gamma_6) - E(\Gamma_8))/\mathrm{d}T$ is deduced instead of a positive one in Ref. [13].

5. Photoemission on HgSe(110)

As discussed by Gawlik [1] the determination of the fundamental bandgap on HgSe(100) by photoemission is

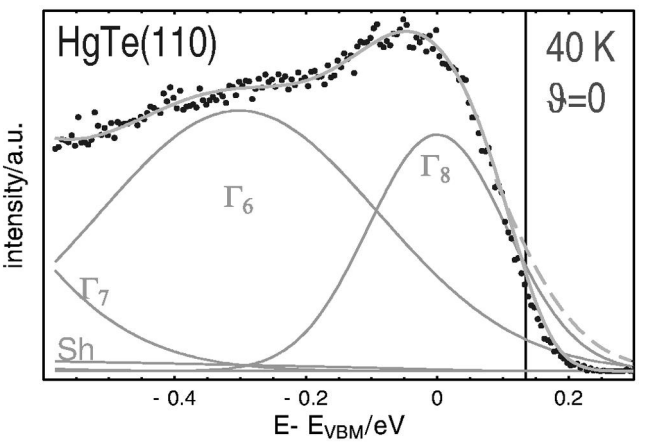

Fig. 4. Energy distribution curve at 40 K and $h\nu = 23$ eV in normal emission together with fit results obtained by a least squares fit. Thin lines are due to a Shirley background, the Gaussians, the fit result with (drawn thin line) and without (broken thin line) the incorporation of the Fermi distribution function.

complicated by emissions, that are due to the band bending on a polar surface. On the non-polar HgSe(110) surface on the other hand this is not to be expected. However, it must be mentioned, that the LEED pictures on this surface are of poorer quality than that from the HgTe(110) surface.

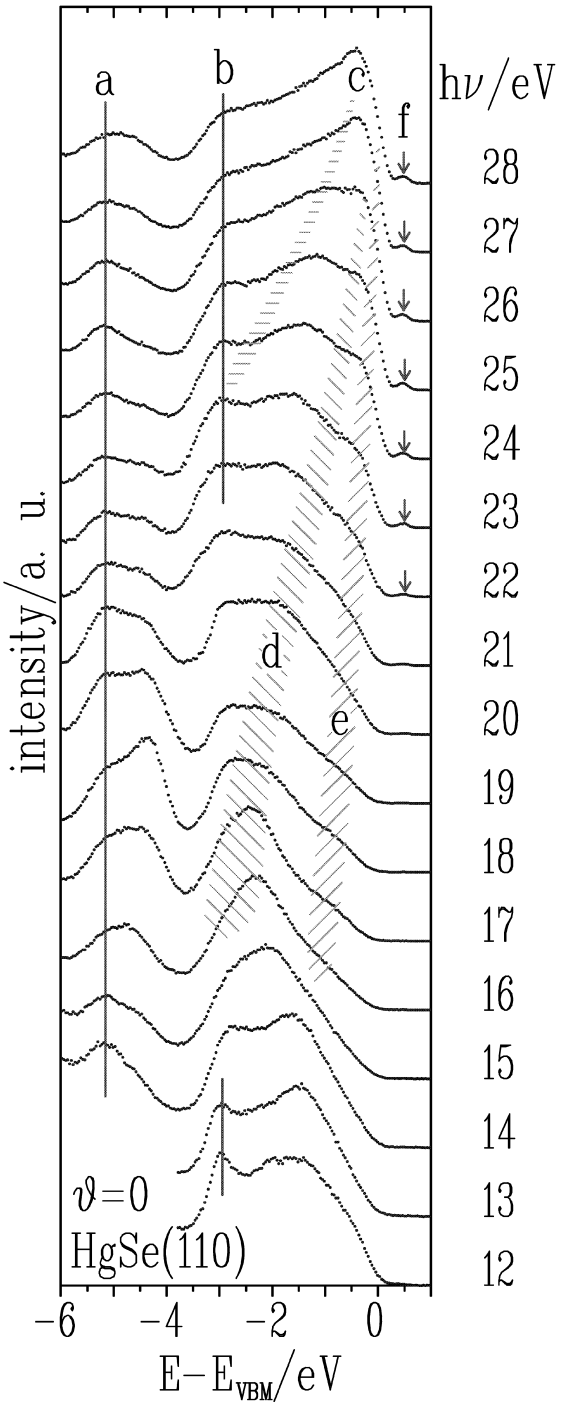

Fig. 5. Energy distribution curves in normal emission of HgSe(110). The shaded structures show dispersion and are related to bulk state emissions, straight lines denote surface state derived features. Structure f is discussed in the text.

Fig. 5 shows a series of photoemission spectra in normal emission. The spectra were fitted as described above and the peak positions were depicted as an experimental band structure in Fig. 6.

The optimum correspondence with the theoretical band structure was obtained for an inner potential of 9 eV, with the valence band maximum occurring at $h\nu = 28$ eV. The experimental band structure was drawn by the reciprocal lattice vectors G = $2\pi/a(220)$, $2\pi/a(111)$, $2\pi/a(200)$, and $2\pi/a((201))$. While the first three are reciprocal bulk lattice vectors, the last G contains additionally a reciprocal surface lattice vector. Dispersing structures attributed to transitions involving G = $2\pi/a(220)$ are labeled by 'c', 'd' and 'e' and are marked as hatched area. Especially the heavy and light hole band can be traced over a wide range. For lower energies the other G's become more important. The structures attributed to the Γ_7X_7-band are not very pronounced, resulting in more uncertainty for this band. The position of the *X*-point was determined to be −5.2 eV, with the dispersionless structure 'a' defining the lower valence band minimum. The dispersionless structure 'b' at −2.9 eV binding energy is attributed to the high density of states at the Σ_1^{min}-point. The experimental band structure reproduces the theoretical band structure of Vogel [11], although an inverted band structure as for HgTe(110) can not be established directly. Structure 'f' at the Fermi energy 0.47 eV above the valence band maximum is comparable in its energy position with the positive energy gap of 0.42 eV found on HgSe(100) [1]. Structure 'f' shows no dispersion and can therefore not be ascribed to the strongly dispersive conduction band. On the other hand the structure disappears when lowering the photon energy below $h\nu = 19$ eV. This behaviour is unusual for a true surface state, which should be observable for all photon energies. Additionally, structure 'f' disappears for off-

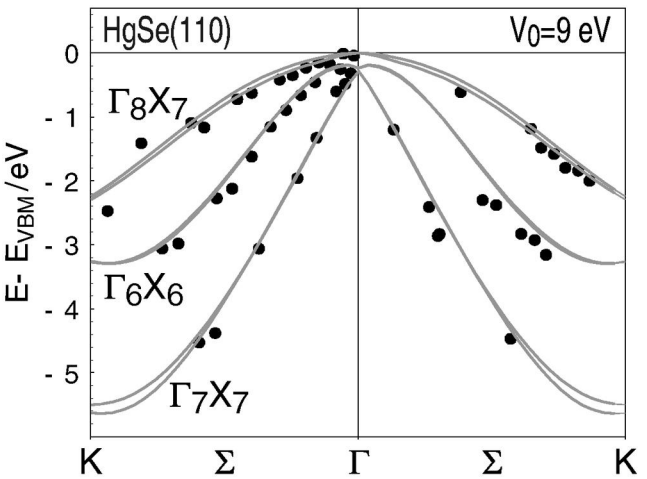

Fig. 6. Experimental band structure of HgSe compared with an ab initio calculation.

normal emission and reappears at the next surface Γ-point, making an interpretation as surface state plausible. These findings must be interpreted in the context of the poorer surface quality and the concentration of doping atoms.

6. Discussion

The interpretation of the data on HgTe is straightforward and proves the inverted band structure for this material. The size of the negative bandgap and the spin–orbit splitting are in favorable agreement with optical measurements. The center of gravity of the leading peak Γ_8, i.e. the valence band maximum, is found 0.1 eV below the Fermi energy, its onset reveals at Γ a Fermi–Dirac-cutoff. This cutoff is an additional strong hint for the inverted band structure, where the gap at E_F should be zero. The difference between VBM and E_F is not due to experimental uncertainties but instead points to a partially occupied conduction band. The mercury based II–VI-semiconductors show self-intercalation effects, generating a small amount of excess charge. The band mass of the conduction band is 0.03 electron masses and small compared to the bandmass of 0.4 eV of the heavy hole band. As the unfilled density of states is therefore very small, the only observable effect is the shift of E_F.

The interpretation of the results on HgSe(110) is more complicated. Since the spin–orbit splitting at Γ is just 0.3 eV, it was impossible to resolve all three bands as in the case of HgTe. Instead these bands could be proven by following their dispersion over the whole Brillouin zone. Nevertheless the Γ_8 valence band maximum is separated from the Fermi level by approximately 400 meV. Additionally at the Fermi edge an additional weak structure appears, which can neither be assigned unequivocally to the conduction band minimum nor to a true surface state. The surface quality seems to be of crucial importance for this material. Part of the observations may be due to inhomogenities in the crystal structure. In any case for the (110)-face of HgSe similar effects as on the (100)-face may be present. Therefore possibly a bulk emission is masked by surface-derived states. Further improvement may come from measurements on differently prepared surfaces, for instance by molecular beam epitaxy. This may also give additional information, to what extent the observed electronic structure is due to the special conditions on the surface and to what extent true bulk states are observed.

Although the results are not satisfying with respect to these problems, the overall experimental band structure is in good agreement to theory regarding band dispersion and bandwidth.

Orlowski et al. [9] have studied the effect of iron on the valence band structure of HgSe. Their spectra of HgSe(110) in normal emission show also a valence band maximum at 28 eV, but with an inner potential of -11 eV. These authors do not observe a structure at E_F like emission ‘f’ in our measurements. Instead for $Hg_{0.87}Fe_{0.13}Se$ a contribution of the iron–DOS approximately 0.3 eV above the valence band maximum is detected. A common origin of these structures however is less plausible since the Fe concentration is lower by a factor of 43 in our samples.

7. Summary

The electronic band structure derived from the spectra agrees well with theoretical data in the case of HgTe(110). The photoemission results especially at the valence band maximum prove that HgTe(110) has really a negative energy gap and inverted band structure.

However, big difficulties in interpretation appear in the case of the HgSe(110) surface. Because of narrow spin–orbit splitting of Se atoms as compared to Te atoms the individual bands at the valence band maximum could not be resolved. At locations in *k*-space with larger separation of the states, three bands as claimed by theory could nevertheless be detected. Additionally, the spectra for HgSe(110) have weak structures in the vicinity of the valence band maximum at the Fermi energy, whose surface or bulk origin could not be determined unequivocally. At present it can therefore not be decided, whether they are true bulk features or possibly result from imperfections of cleavage and/or Fe impurities. It is still an open question whether photoemission on the HgSe(110) surface can provide evidence of a negative energy gap.

Acknowledgements

We gratefully acknowledge assistance of the staff of HASYLAB, namely Dr. P. Gürtler and the staff of the WESPHOA spectrometer of the University of Kiel, namely K. Rossnagel. We also thank the staff of BESSY. This work received funding from the Bundesministerium für Bildung, Wissenschaft, Forschung und Technologie (BMBF) under project no. BMBF 05 SB8KH9.

References

[1] K.-U. Gawlik, L. Kipp, M. Skibowski, N. Orlowski, R. Manzke, Phys. Rev. Lett. 78 (1997) 3165.
[2] R. Piotrzkowski, S. Porowski, Z. Dziuba, J. Ginter, W. Giriat, L. Sosnowski, Phys. Status Solidi 8 (1965) K135.
[3] T. Dietl, W. Dobrowolski, J. Kossut, B.J. Kowalski, W. Szuszkiewicz, Z. Wilamowski, A.M. Witowski, Phys. Rev. Lett. 81 (1998) 1535;
K.U. Gawlik, L. Kipp, M. Skibowski, N. Orlowski, R. Manzke, Phys. Rev. Lett. 81 (1998) 1536.
[4] M. von Truchseß, A. Pfeuffer-Jeschke, C.R. Becker, G. Landwehr, E. Batke, Phys. Rev. B 61 (2000) 1666.

[5] M. Rohlfing, S.G. Louie, Phys. Rev. B 57 (1998) R9392.
[6] N. Orlowski, J. Augustin, Z. Golacki, C. Janowitz, R. Manzke, Phys. Rev. B 61 (2000) R5058.
[7] X. Yu, L. Vanzetti, G. Haugstad, A. Raisanen, A. Franciosi, Surf. Sci. 275 (1992) 92.
[8] R. Reifenberger, J. Kossut, J. Vac. Sci. Technol. A5 (5) (1987) 2995.
[9] B.A. Orlowski, J. Bonnet, C. Hricovini, R. Pinchaux, J. Gorecka, B.J. Kowalski, A. Mycielski, Acta Phys. Pol. A80 (3) (1991) 389.
[10] M. Banouni, M. Nasser, G. Leveque, J. Cryst. Growth 159 (1996) 736.
[11] D. Vogel, PhD thesis Westfälische Wilhelms-Universität Münster (1998).
[12] C. Janowitz, L. Kipp, R. Manzke, B.A. Orlowski, Surf. Sci. 231 (1990) 25.
[13] G.L. Hansen, J.L. Schmitt, T.N. Casselman, J. Appl. Phys. 53 (1982) 7099.